ORIGINAL PAPER

Irena Arsova · Ljubomir Arsov · Niels Hebestreit ·
Andreas Anders · Waldfried Plieth

Electrochemical formation of anodic oxide films on Nb surfaces: ellipsometric and Raman spectroscopical studies

Abstract Electrochemical formation of anodic oxide films on niobium (Nb) surfaces in 1 M H_2SO_4 solutions was studied using ellipsometry and Raman spectroscopy. By in situ ellipsometric measurements, the coefficient of film thickness growth and the complex index of refraction of anodic oxide films in the voltage range between 0 and 100 V were determined. The Raman spectra reveal that the thin passive films are amorphous. In the beginning of crystallization, the anodic oxide films consist of mixtures of NbO_2 and Nb_2O_5, while NbO_2 is completely transformed to Nb_2O_5 for thicker and well-crystallized films.

Keywords Niobium oxide · Anodic oxide films · Cyclic voltammetry · Ellipsometry · Raman spectroscopy

Introduction

In recent years, there has been a growing interest in electrochemistry of niobium (Nb) and its alloys. This metal is used in various branches of chemical industry and for mechanical engine constructions. One of the most important applications of Nb is as an alloying element for high-strength low-alloy steels in automobile and for high-pressure gas transmission pipelines. The other important role is to provide creep strength in superalloys operating in the hot section of aircraft gas turbine engines and also in production of superconducting niobium–titanium alloys.

The high corrosion resistance of Nb is based on the spontaneous formation of natural oxide films (thickness 4–6 nm) on its surface at atmospheric condition. The tendency of Nb to form very stable oxygen compounds is related to its negative standard potential of $E_0=-0.96$ V_{NHE} [1].

Anodic oxidation is a well-established procedure in the case of Nb, and recently, several papers were published concerning film thickness growth, studying, e.g., the effect of ion incorporation [2], the field dependence, [3], ionic conductivity [4], and the change in surface properties by cathodic polarization [5]. The anodic oxidation of Nb was generally carried out under galvanostatic conditions at current densities from 0.1 to 10 mA/cm^2. The linear increase of the potential during the galvanostatic oxidation of Nb with 100% current yield indicates the ionic nature of the current passing through the oxide film [6]. So far, a linear relationship of film thickness and anodizing overvoltage was observed with slopes of α=1.9 to 5.0 nm/V [3, 7–9]. The properties of the oxide film with growing thickness were investigated from Badawy et al. (1989) [10] using photoelectrochemical impedance and capacitance measurements in H_2SO_4 and HNO_3 solutions.

The known stable oxides of Nb are NbO, NbO_2, and Nb_2O_5. Using ion scattering spectroscopy, Gray (1975) [11] has shown that the oxide film grown on Nb had a two-layer structure. The external layer was composed of Nb_2O_5 with thickness depending on applied anodic voltage. The inner layer with a thickness of about 5 nm corresponded to metallic NbO. NbO_2 was not found in this investigation.

The goal of this work was to study the dependence of the chemical composition, crystallinity, and optical properties of thicker anodic films on the applied potential. The methods used were Raman spectroscopy and ellipsometry.

Experimental

Electrodes Working electrodes were prepared from annealed 99.8% niobium rod 6.35 mm in diameter (Alfa Aesar, JMC, USA). The sides of the rods and one basic plane were isolated by epoxy resin (Struers), while the other basic plane with the constant surface area of 31.6 mm^2 was in contact with the electrolyte serving as working electrode. Depending on the experimental technique, two types of surface preparation were performed. In

I. Arsova · L. Arsov
Faculty of Technology and Metallurgy,
University "St. Cyril and Methodius",
1000 Skopje, Macedonia

N. Hebestreit (✉) · A. Anders · W. Plieth
Institut fur Physikalische Chemie und Elektrochemie,
TU Dresden, Germany
e-mail: niels.hebestreit@chemie.tu-dresden.de

one case, the electrode surface was grinded with a set of emery papers (from 600 to 5,000 grain size), mirror-polished with diamond spray (from 6 to 0.1 μm), and carefully ultrasonically degreased in acetone and ethyl alcohol. This kind of preparation was used in Raman spectroscopic measurements. In the second case, the electrode surface was mechanically polished with emery paper 600 and then electropolished in a bath of 170 ml HNO_3 + 50 ml HF + 510 ml CH_3OH + 5 g citric acid at a voltage of 15.2 V for 1 min under strong stirring and at a temperature of −5°C. Finally, the electrodes were rinsed with distilled water and ultrasonically treated in ethyl alcohol. This kind of preparation was used for ellipsometric measurements. The quality of electropolishing was tested ellipsometrically.

After finishing a measurement, no extensive mechanical repolishing was necessary.

Cells For ellipsometric in situ measurements, a special optical electrolytic cell with two optical quartz windows fixed at an angle of 70° was adopted. The specimen surface was mounted vertically, with a rigid clamping system having adjustments for rotation, tilt, and central positioning in the cell. Details of the design of this optical electrolytic cell are given elsewhere [12].

Solutions One molar solution of sulfuric acid was prepared from concentrated H_2SO_4 (Merck, extra pure), with triply distilled and deionized water. The electrolyte in the cell was changed after each measurement to avoid eventual build up of concentrations of soluble Nb species.

Apparatus, procedure of measurements For ellipsometric measurements the anodic polarization was performed potentiostatically, using HEKA Model 488 potentiostat/galvanostat connected to a personal computer. The voltage was increased stepwise every 30 s by 0.5 V from 0 to 10 V. For voltages up to 10 V, a three-electrode system was used. For voltages >10 V, a two-electrode system was used, and the applied voltage was increased in steps of 2.5 V every 30 s from 10 to 100 V. After each experiment, a new electrode was prepared. The ellipsometric measurements were performed with a "thin film ellipsometer, Rudolph Research, type 43603-200" at a wavelength of λ=546.1 nm and at an incidence angle of φ=70°.

Electrodes for Raman spectra measurements, mechanically polished to mirror brightness, were anodized every 30 s at various voltages, up to 150 V. Raman spectra were recorded with a "Renishaw Ramascope" using a red laser (633 nm) at a power of 1 mW.

Results

For thicker anodic films, usually the formation of Nb_2O_5 is assumed by the reaction

$$2Nb + 5H_2O \rightarrow Nb_2O_5 + 10H^+ + 10e^-. \qquad (1)$$

To determine the film thickness, several techniques have been used in the literature: differential capacitance measurements [13], measurement of the total amount of charge used in the film formation [14], spectrophotometric techniques [14], and ellipsometry [4, 15]. From all these methods, ellipsometry is the most exact method in determining the thickness d and the optical constants [refractive index (real part) n, refractive index (imaginary part, extinction coefficient) κ].

Exact determination of these parameters require a preliminary knowledge of the refractive indices of the bare metal $\widehat{n}_s = n_s(1 - i.\kappa_s)$ and surrounding media $\widehat{n}_m = n_m(1 - i.\kappa_m)$. A principal problem is how to determine the refractive indices of the bare metal substrate without presence of any surface oxide film. One technique for determining optical indices of bare metal substrates is evaporation of metal in vacuum then measurement is done under high-vacuum condition.

However, the refractive indices of evaporated films will differ from the values of bulk metals. A compromise is to measure the electrolyte with oxide films at different potentials (thicknesses) and to extrapolate to zero thickness. In the literature, data determined in this manner show big discrepancies in the values of the refractive indices. For λ=546.1 nm and films grown in 1 M KCl and 2 N H_3PO_4, Li and Young (2000) [2] published a value of $\widehat{n}_s = 3.17$ $(1 - 1.132 \cdot i)$ by fitting substrate and oxide refractive indices. For a film grown in 0.1 M H_2SO_4 and using the same fitting procedure, Young and Zobel (1966) [4] found for electropolished Nb, a value of $\widehat{n}_s = 3.6(1 - 1 \cdot i)$. At the same wavelength for mechanically polished Nb, (polished with alumina powder, 5–30 nm particle diameter) Dyer and Leach (1978) [16] found the very low value of $\widehat{n}_s = 2.85$ $(1 - 1.105 \cdot i)$.

In this work, for determining the refractive indices of electropolished oxide-free Nb surfaces, the fitting procedure of experimentally determined $\psi - \Delta$ values in 1 M H_2SO_4 at relatively low anodic potentials (from steady-state potential up to 5 V NHE) with theoretical $\Delta - \psi$ plots calculated from Fresnel's equation for a three-component system (medium, oxide film, metal substrate) were used [17].

The ellipsometric parameters ψ and Δ in Fresnel's equation are related with reflection coefficient r_p for light polarized parallel and coefficient r_s for light polarized perpendicular to the plane of incidence.

$$\text{tg}\psi \cdot \exp(i \cdot \Delta) = \frac{r_p}{r_s} \qquad (2)$$

For a three-component system, the ellipsometric parameters ψ and Δ are complex functions of the following parameters

$$\text{tg}\psi \cdot \exp(i \cdot \Delta) = (\widehat{n}_m, \widehat{n}_f, \widehat{n}_s, d, \lambda, \varphi). \qquad (3)$$

To minimize the unknown parameters in Fresnel's equation, the refractive index of the medium was determined by an Abbe refractometer.
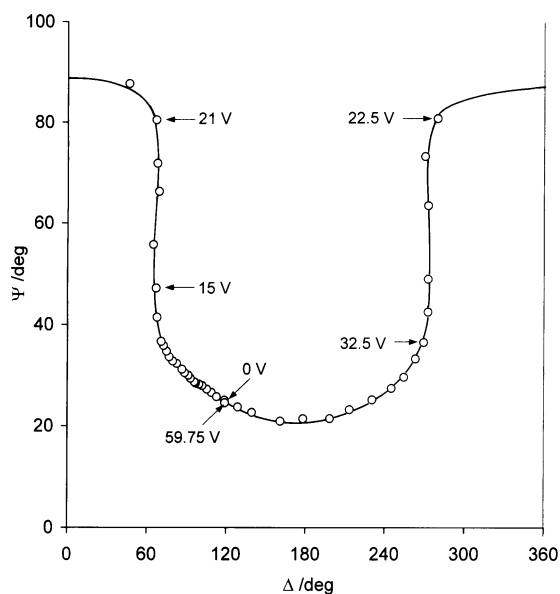
For 1 M H₂SO₄ at room temperature of 20°C, $\widehat{n}_m = 1.3442(1 - 0 \cdot i)$, i.e., n_m=1.3442 and κ_m=0 was found. These values are in good agreement with the values of n_m given for 1 M H₂SO₄ in Weast RC (1975) Handbook [18]. Utilizing the described fitting procedure, a complex refractive index of $\widehat{n}_s = 3.62(1 - 0.993 \cdot i)$ [17] was determined for Nb. This value was used in all further evaluations of ellipsometric data. The ellipsometric data obtained during the anodic oxidation of Nb are shown in Fig. 1.

When the working electrode was polarized at potentials higher than 2 V (NHE), oxygen bubbles had to be avoided. Each potential was applied for 30 s, then the potential was switched back to 2 V (NHE), were the residual anodic current was too small for gas evolution.
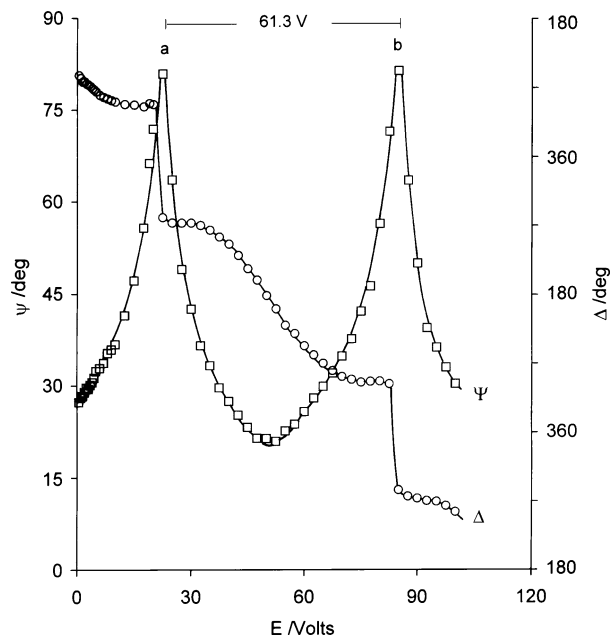
The curve through the experiment points in Fig. 1 is obtained by fitting the data for a film of index $\widehat{n}_f = 2.345$ $(1 - 0.0005 \cdot i)$. The fitting procedure was performed by searching $\widehat{n}_f$ in the theoretical Fresnel's curve for the prior given values of the thickness in increments of 1 nm in an increasing direction. The relatively good superposition of the experimentally measured points with theoretically fitted curve gained from this curve a precise determination of $\widehat{n}_f$ and coefficient of film thickness growth α. Details of the computer program and the fitting procedure are given in Efremova and Arsov (1992) [19].

Analyzing the data of Fig. 1 at a voltage of 59.75 V, the experimentally measured $\psi - \Delta$ data are identical to the $\psi_o - \Delta_o$ values calculated for the bare metal. The data at 59.75 V correspond to a film thickness of d=138 nm. The $\psi - \Delta$ data are cyclic functions of the thickness because the imaginary part of the refractive index is very small, nearly zero.

For precise calculations of the coefficient of the film thickness growth, the experimental and theoretical ψ and Δ data vs applied potential shown in Fig. 2 were used.
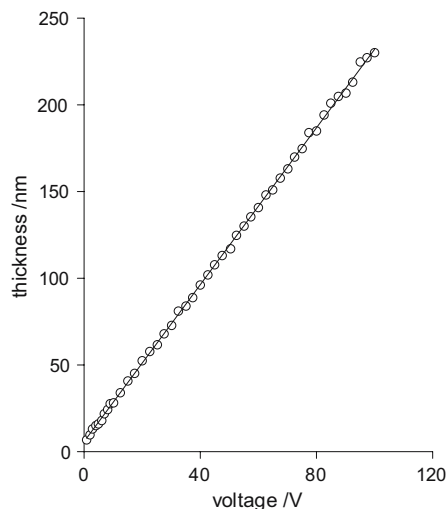

Fig. 2 Graphical plot of experimentally measured ellipsometric Δ (o) and Ψ (□) parameters in dependence of applied voltage for anodically polarized Nb electrodes in 1 M H₂SO₄. *Lines* represent theoretically fitted curves

From Fresnel's equation and assuming that κ_f=0 (film is nonabsorbing), one obtains

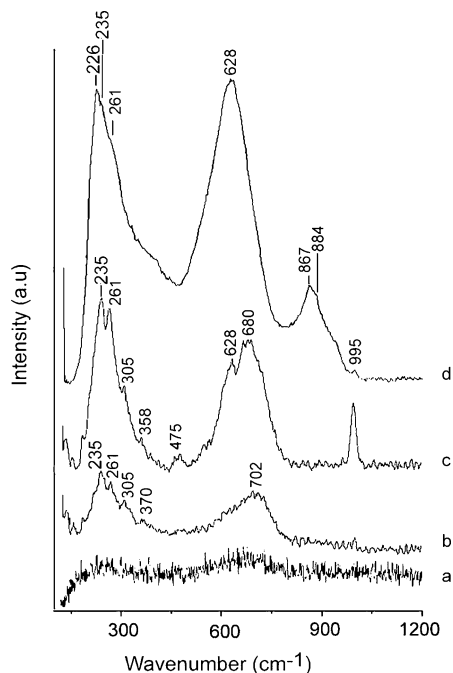$$\delta = \frac{2 \cdot \pi}{\lambda} \cdot d \cdot \left(\widehat{n}_f^2 - \widehat{n}_m^2 \cdot \sin^2 \varphi \right)^{1/2} \quad (4)$$

with δ as phase change of the beam crossing the film (thickness d), λ wavelength, $\widehat{n}_f$, and $\widehat{n}_m$ complex refractive index of film and surrounding medium, respectively. Angle of beam incidence is represented by φ (φ=70°).

The ψ vs E and Δ vs E plots show two singularities (a) and (b), corresponding to a phase change of δ=180°. As

Fig. 1 Graphical plot of ellipsometric $\psi - \Delta$ data, of anodically filmed Nb electrodes for various voltages in 1 M H₂SO₄. *Circle* represents experimentally measured data; *line* represents theoretically fitted curve

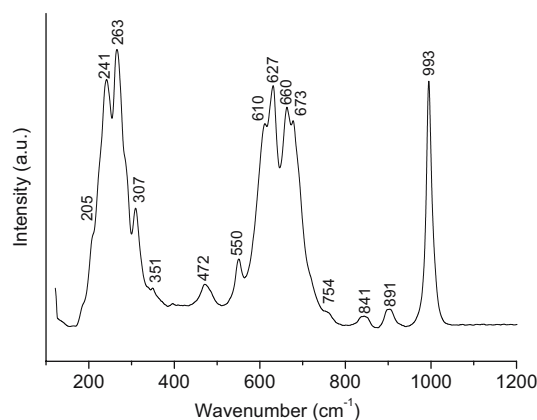**Fig. 3** Film growth on an electropolished Nb electrode in 1 M H₂SO₄; thickness vs applied voltage

Fig. 4 Raman spectra of mechanically polished Nb electrodes anodically polarized in 1 M H_2SO_4 at various voltages film formed at **a** 15 V, **b** 30 V, **c** 80 V, and **d** 150 V

Fig. 5 Raman spectra of Nb_2O_5 powder at room temperature

can be seen from Fig. 2, there is a fairly good agreement between the experimental data and the theoretically fitted curve. From the voltage distance of 61.3 V between the singularities and the corresponding difference of thickness of 138.5 nm, the calculated coefficient of film thickness growth is $\alpha = 2.26$ nm/V. This coefficient of film thickness is obtained for anodic voltage growth only, without any contribution of the natural oxide film.

The film thickness as a function of the applied voltage, is shown in Fig. 3.

With extrapolation to 0 V, a thickness of about 5 nm of the natural oxide film can be determined.

Raman spectroscopy Raman spectroscopy is an alternative technique to the standard X-ray and electron diffraction techniques to study crystal structure. So far, a series of niobium oxide reference compounds was investigated by Raman spectroscopy to determine the relationship between the niobium oxide structure and the corresponding Raman spectra [20, 21].

The Raman spectra of anodic oxide films on Nb formed at various voltages are shown in Fig. 4. The characteristic Raman bands are listed in Table 1.

In Fig. 5, the Raman spectrum of powdered Nb_2O_5 as a reference spectrum is shown. It was not possible to record the Raman spectrum of powdered NbO_2 due to its dark color.

Characteristics of Raman bands for various polymorph forms of Nb_2O_5 from literature are also listed in Table 1.

For the natural oxide film and up to 10 V, no Raman bands could be observed. For anodic voltage of 15 V, two broad bands located at 234 and 702 cm^{-1} appear (Fig. 4a). Increasing the potential, the bands rise in intensity and additional bands located at 261, 305, and 370 cm^{-1} appear (Fig. 4b). At 80 V (Fig. 4c), the Raman spectrum is

Table 1 Observed Raman frequencies for niobium oxides

Compound	Raman bands (cm^{-1})	Reference
H–Nb_2O_5	995(s), 883(m), 670(m), 625(s), 550(w), 470(w), 350(w), 260(s), 232(s), 204(m)	[20]
N–Nb_2O_5	995(s), 885(m), 670(m), 618(s), 550(w), 485(w), 350(w), 260(s), 220(m)	[20]
B–Nb_2O_5	935(w), 760(s), 625(m), 605(m), 550(s), 475(m), 450(m), 370(s), 260(s), 200(s)	[20]
Nb_2O_5	996(s), 904(w), 848(w), 664(s), 632(s), 552(w), 472(w), 350(w), 308(m), 264(s), 240(s)	[27]
NbO_2	704(m,b), 476(w), 392(w)	[27]
Nb electrochemically 30 V	702(s,b), 370(w), 305(w), 261(w), 235(m)	This work
Nb electrochemically 80 V	995(s), 680(s,b), 628(m), 475(m,b), 358(w), 305(w), 261(w), 235(m)	This work
Nb electrochemically 150 V	995(m), 884(w), 867(m), 628(s), 261(sh), 235(sh), 226(s)	This work
Nb_2O_5 powder	993(s), 891(m), 841(w), 754(sh), 673(s), 660(s), 627(s), 610(m), 550(m), 472(m), 351(w), 307(m), 263(s), 241(s), 205(sh)	This work

s Strong, *m* medium, *w* weak, *sh* shoulder, *b* broad

changing. The band at 702 cm^{-1} characteristic for NbO_2 is split into two new bands located at 628 and 680 cm^{-1} tentatively assigned to the transformation of NbO_2 to the Nb_2O_5. At 150 V (Fig. 4d), relatively strong bands at 226 and 628 cm^{-1}, medium bands at 884 and 995 cm^{-1} and a shoulder on 261 cm^{-1} can be attributed to Nb_2O_5.

Discussion

In the literature, big discrepancies about the electrochemical properties and the structure of passive and anodic films (especially of thin films) exist [2, 3, 6, 22, 23]. To analyze the surface oxide film by ellipsometry, the complex refractive index of the substrate metal must be known. As shown in previous work, an incorrect determination of the optical constants of the bare substrate is one of the main sources of the essential errors in ellipsometric measurements [19]. The surface preparation strongly affects the optical constants of the substrate varying from $\widehat{n}_s = 2.85$ $(1 - 1.105 \cdot i)$ to $\widehat{n}_s = 3.6(1 - 1 \cdot i)$ [16, 4]. The other source of error in ellipsometric measurements, not pointed out sufficiently in the literature, is that the thickness–voltage dependence was always determined for high-voltage oxides. The thickness–voltage relationship can change during the growth of the oxide. Moreover, aging phenomena might occur. It should be pointed out that it is still an open question to carry out the analysis of ellipsometric data [15, 24] with a one-layer or a two-layer model.

Lee et al. (1974) [15] fitted their ellipsometric data with a two-layer model: an outer layer with n=2.15 and an inner layer with n=2.37. The thickness of the outer layer was 40% of the total thickness. Later, Knorr and Leslie (1974) [24] criticized this model, evaluating data by a one-layer model.

It is evident from Figs. 1 and 2 that our experimental data very well confirm the one-layer model. Of course, this is no proof that underneath the thicker "bulk" oxide film, a thin layer of metal rich niobium oxide exists. There is no evidence that the anodic oxide film formed on Nb in H_2SO_4 consists of two distinct layers.

Concerning the oxide film structure, most of the niobium oxide compounds contain a disturbed Nb–O octaeder structure. The niobium oxide compounds with a tetrahedral structure are extremely rare. All Raman band assignments for anodic oxide films are based on the corresponding Nb–O bond. According to literature data, all Raman bands in the 200–300 cm^{-1} wave number region are assigned to the bending modes of the Nb–O–Nb bond [20, 21]. The associated symmetric and antisymmetric stretching modes appear in the higher wave number region (400–800 cm^{-1}). The wave number region from 800 to 1200 cm^{-1} is characteristic for the symmetric and antisymmetric stretching modes of the Nb=O terminal double bond in the structure of Nb_2O_5.

Niobium pentoxide Nb_2O_5 can exist in different polymorphic forms (H–Nb_2O_5, N–Nb_2O_5, and B–Nb_2O_5). Its phase transformations strongly depend on the heat treatment [20]. Thermodynamically, the most stable form of the Nb_2O_5 oxides is H–Nb_2O_5 formed at about 1,000°C having the highest bond order [25]. The polymorphism of Nb_2O_5 phases are confirmed by X-ray diffraction and metallographic studies [21, 26]. $Nb_2O_5 \cdot nH_2O$ existing up to 120°C is found to be nearly amorphous, showing a diffuse X-ray pattern.

Comparing the characteristic Raman bands in Fig. 4 with literature data listed in Table 1, it is evident that for thinner films no active bands were monitored, confirming the amorphous structure of the passive film. On the contrary, Huang et al. (1999) [27] utilizing the surface enhanced Raman spectroscopy effect, after Ag coating of the electrode surface, found Raman bands of Nb electrochemically treated in 0.15 m NaCl at potentials −0.4 V, OCP and 0.4 V vs Ag/AgCl. According to these authors, the passive film is composed of NbO_2 mixed with different forms of Nb_2O_5. Some of the bands in our paper deviate from the Raman bands of [27].

For thicker anodic films, the Raman spectra show well-defined Raman bands, indicating increase of film crystallinity with applied voltage. For lower anodic voltages, the oxide film is composed of NbO_2 and Nb_2O_5. The band at 235 cm^{-1} is a fingerprint for H–Nb_2O_5, and the band at 702 cm^{-1} is characteristic for NbO_2 [27]. The apparition of first Raman bands in Fig. 4 is in close relation to breakdown processes. During the anodic polarization, the current was oscilloscopically monitored showing small fluctuations at 15 V and large oscillations at 150 V. Up to 150 V, no thermal effects as a result of current breakdowns or the existence of sparks were observed.

Conclusion

The following conclusions can be drawn:

- The thickness of anodic oxide films on Nb in 1 M H_2SO_4 increases linearly with the applied potential. The coefficient of film thickness growth is 2.26 nm/V.
- The one-layer model was successfully used for the evaluation of ellipsometric data and a refractive index n_f=2.345(1−0.0005i) in the voltage range from 0 to 100 V was calculated. The very low value of the index of adsorption indicates that the film is transparent.
- The chemical composition of anodic oxide films of Nb at the beginning of crystallization is a mixture of NbO_2 and Nb_2O_5. As crystallization progresses, NbO_2 transforms into Nb_2O_5.

214

References

1. Van Muylder J, De Zubov N, Pourbaix M (1957) Comportment electrochemique du niobium. Diagramme d,equilibres tension-pH du sysetme Nb–H2O a 25°C (Rapport technique RT-53 of CEBELCOR, June 1957)
2. Li YM, Young L (2000) J Electrochem Soc 147(4):1344
3. Ord JL, Hopper MA, Wang WP (1972) J Electrochem Soc 119:439
4. Young L, Zobel F (1966) J Electrochem Soc 113:227
5. Vaskevich A, Rosenblum M, Gileadi E (1995) J Electrochem Soc 142:1501
6. Young L (1956) Trans Faraday Soc 52:515
7. Juliao JF, Chagas JW, Cesar HL, Dias NL, Decker F, Gomes UU (1991) Electrochim Acta 36:1297
8. Davydov AD, Kamkin AN (1981) Elektrokhimiya 17:1243
9. Makara EV, Mikhalkin VS, Odynets LL (1971) Elektrokhimiya 7:1096
10. Badawy WA, Felske A, Plieth WJ (1989) Electrochim Acta 34:1711
11. Gray KE (1975) Appl Phys Lett 27:462
12. Arsov LJ (1985) Electrochim Acta 30:65
13. Gomes MA, Bulhoes JS, De Castroud SC, Damiao AJ (1990) J Electrochem Soc 137:3076
14. Goswani A, Goswani AP (1975) J Appl Phys 13:667
15. Lee WL, Oliva G, Pulfrei DL, Young L (1974) J Electrochem Soc 117:1272
16. Dyer CK, Leach JS (1978) J Electrochem Soc 125:23
17. Arsova I, Prusi A, Arsov LJ (2003) J Solid State Electrochem 7:217
18. Weast RC (1975) Handbook of chemistry and physics, 56th edn. CRC, Cleveland, OH
19. Efremova A, Arsov LJ (1992) J Phys II France 2:1353
20. McConnell AA, Anderson JS, Rao NR (1976) Spectrochim Acta 32A:1067
21. Jehng JM, Vachs IE (1991) Chem Mater 3:100
22. Piazza S, Sunseri C, Di Quarto F (1990) J Electroanal Chem 293:69
23. Sugimoto K, Belanger G, Piron LD (1979) J Electrochem Soc 126:535
24. Knorr K, Leslie JD (1974) J Electrochem Soc 121:805
25. Sheasby JS, Wallwork GR, Smeltzer WW (1966) J Electrochem Soc 113:1255
26. Sheasby JS (1968) J Electrochem Soc 115:695
27. Huang BX, Wang K, Church JS, Li YSW (1999) Electrochim Acta 44:2571